Steps Control the Dissociation of CO2 on Cu(100)

JACS JOURNAL OF THE AMERICAN CHEMICAL SOCIETY

Article

Cite This: J. Am. Chem. Soc. 2018, 140, 12974−12979

pubs.acs.org/JACS

Steps Control the Dissociation of CO_2 on Cu(100)

Benjamin Hagman,[†,#] Alvaro Posada-Borbón,[‡,#] Andreas Schaefer,[§] Mikhail Shipilin,[∥] Chu Zhang,[†] Lindsay R. Merte,[⊥] Anders Hellman,[‡] Edvin Lundgren,[†] Henrik Grönbeck,[‡] and Johan Gustafson*[,†]

[†]Synchrotron Radiation Research, Lund University, Box 118, 221 00 Lund, Sweden

[‡]Department of Physics and Competence Centre for Catalysis, and [§]Department of Chemistry and Chemical Engineering and Competence Centre for Catalysis, Chalmers University of Technology, 412 96 Gothenburg, Sweden

[∥]Department of Physics, AlbaNova University Center, Stockholm University, 106 91 Stockholm, Sweden

[⊥]Department of Materials Science and Applied Mathematics, Malmö University, 205 06 Malmö, Sweden

Supporting Information

ABSTRACT: CO_2 reduction reactions, which provide one route to limit the emission of this greenhouse gas, are commonly performed over Cu-based catalysts. Here, we use ambient pressure X-ray photoelectron spectroscopy together with density functional theory to obtain an atomistic understanding of the dissociative adsorption of CO_2 on Cu(100). We find that the process is dominated by the presence of steps, which promote both a lowering of the dissociation barrier and an efficient separation between adsorbed O and CO, reducing the probability for recombination. The identification of steps as sites for efficient CO_2 dissociation provides an understanding that can be used in the design of future CO_2 reduction catalysts.

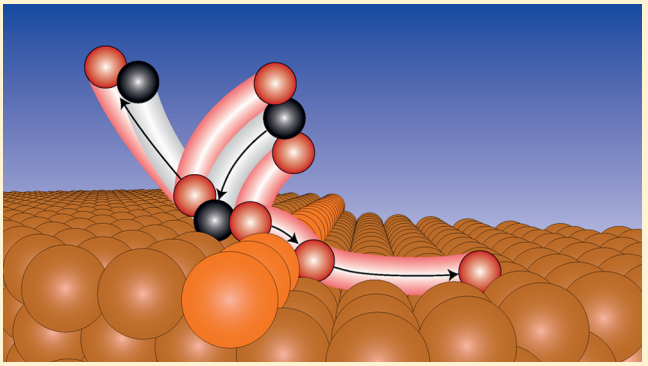

1. INTRODUCTION

Because of global warming, there is a strong need to reduce emissions of greenhouse gases, such as CO_2, into the atmosphere. In the case of CO_2, one possible path is to convert the molecule into useful chemicals, such as methanol. The approach to recycle CO_2 will not only reduce the issues with global warming but also provide a closed carbon loop for production of essential chemicals.[1,2]

Recycling of CO_2 is challenging because of the inertness of the molecule with high barriers for activation. To promote the development of new catalysts, it is desirable to have a fundamental understanding of the activation and dissociative adsorption of CO_2 on relevant surfaces. Industrially, Cu-based catalysts, especially combined with ZnO, play an important role for both the reversed water−gas shift reaction and methanol synthesis from CO_2. The roles of the Cu, ZnO, and Cu/ZnO interface have been discussed during the last 2 decades.[3−9] To reach a fundamental understanding of the reaction process, it is important to study the two components also individually. Thus, the interaction and dissociation of CO_2 on copper and copper oxide surfaces have received considerable attention.[10−22]

Rasmussen et al. observed CO_2 dissociation on Cu(100) at close to atmospheric pressures and at temperatures between 475 and 550 K.[10] Exposure to CO_2 left adsorbed oxygen on the surface, while the CO resulting from the dissociation desorbed. The determined[10] dissociative sticking coefficient of CO_2 was on the order of 10^{-12}. This implies that any in situ experiments need to be performed at elevated pressures to be able to observe adsorbed oxygen. Ambient pressure X-ray photoelectron spectroscopy (AP-XPS) has made it possible to study the dissociative adsorption of CO_2 on copper surfaces at elevated pressures, which is not possible with traditional XPS.

Using AP-XPS, Eren et al. have shown that CO_2 adsorbs dissociatively on Cu(100) at pressures in the range 0.1−10 mbar at 300 K.[11] Chemisorbed $CO_2^{\delta-}$ as well as adsorbed atomic oxygen were observed on the surface. Furthermore, at a coverage of 0.3 ML (MonoLayers, 1 ML = 1.53×10^{15} cm^{-2}), adsorbed oxygen was found to hinder the adsorption of CO_2, which emphasizes the need of CO in the gas mixture to remove the chemisorbed oxygen. However, the knowledge of how CO_2 interacts with pristine and oxygen-covered Cu(100) is limited and there is a need for uncovering the role of surface oxygen in this process.

We have studied the dissociative adsorption of CO_2 on Cu(100) using AP-XPS and density functional theory (DFT) calculations. In contrast to previous studies, we continuously followed the evolution of the oxygen layer, which allows for a deeper understanding of the dissociation process. In agreement

Received: July 25, 2018
Published: September 18, 2018

with previous studies,[10,11] we find that CO_2 dissociates on the surface, resulting in adsorbed O, and that the rate of dissociation drops as the oxygen coverage approaches 0.25 ML. Interestingly, we find that the oxygen uptake curve is linear with different slopes in the coverage ranges of 0−0.25 and 0.25−0.45 ML. This suggests that the adsorption is unaffected by the O coverage within these ranges. To explain this behavior, we propose a model where steps dominate the CO_2 dissociation process. The calculations show that the effect of the steps is twofold; it both lowers the dissociation barrier and provides an efficient separation between adsorbed O and CO, reducing the probability for the back reaction of CO_2 formation.

2. METHODS

2.1. Sample Preparation. The Cu(100) surface was cleaned by cycles of argon ion bombardment at 1 kV, 10 mA, and 2×10^{-6} Torr for 20 min and subsequent annealing to 850 K for 20 min. The surface was considered clean when only copper was detected in the XPS.

To obtain a calibration of the oxygen coverage, the O 1s peak of the missing row (MR) structure,[23] which contains 0.50 ML of oxygen, was used as reference. This structure was prepared by saturating the clean surface with oxygen by exposure to 1200 L of O_2 at 370 K, which according to scanning tunneling microscopy (STM) and low-energy electron diffraction (LEED) gives the MR structure; see Supporting Information.

2.2. XPS Measurements. The AP-XPS experiments were conducted at Beamline 9.3.2 of the Advanced Light Source at Lawrence Berkeley National Laboratory.[24] The C 1s and Cu 3p spectra were measured using a photon energy of 435 eV, while O 1s was measured at 650 eV. The evolution of the oxygen coverage was monitored by measuring the O 1s region continuously, while the Cu(100) surface was exposed to 300 mTorr CO_2 at 370 K. As the surface is exposed to CO_2, adsorbed atomic oxygen appears on the surface, which originates from the following sequence of reactions:

$$CO_2(g) + * \leftrightarrows CO_2* \quad (1)$$

$$CO_2* \leftrightarrows O* + CO* \quad (2)$$

$$CO* \leftrightarrows CO(g) + * \quad (3)$$

We exclude that the oxygen uptake originates from residual O_2 gas because the observed oxygen uptake curve does not match the expected signature from O_2 gas.[25] After the O 1s signal saturated, the CO_2 was pumped out and O 1s, Cu 3p, and C 1s spectra were measured. The O 1s signal at UHV is then compared to the O 1s signal of the MR to achieve an oxygen coverage calibration.

The series of O 1s spectra was deconvoluted by fitting each peak using a Doniach-Šunjić function convoluted with a Gaussian as well as a linear background. After determination of the positions and line shapes of all the components, the fitting of the spectra was carried out by fixing all parameters except the intensity of the peaks. In this way, the description of the system is consistent for the entire series of spectra. For the peaks at 530.0 and 529.5 eV, the determined asymmetry parameter and fwhm of the Gaussian are 0.098 and 0.86 eV, respectively.

2.3. DFT Calculations. The calculations were performed within density functional theory (DFT) using PBE exchange-correlation functional[26] as implemented in the Vienna ab initio package[27−30] and described in ref 23. Carbon, oxygen, and copper were treated with 4, 6, and 11 electrons in the valence, respectively. The (100), (611), and Cu(11 1 1) surfaces are modeled with slabs consisting of four (100) and five (stepped) layers separated by at least 15 Å of vacuum. For the (100) [stepped] surface, the top two [three] layers were allowed to relax in response to adsorption, whereas the bottom two layers were kept fixed at the bulk positions.

The calculated lattice constant of Cu in fcc bulk is 3.637 Å, in good agreement with the experimental value of 3.615 Å.[31] The bond lengths for carbon dioxide and carbon monoxide in gas phase are calculated to be 1.18 and 1.14 Å, respectively. This is close to the experimental values of 1.16 and 1.13 Å.

Reaction barriers were calculated using the climbing-image nudged elastic band (CI-NEB) technique as implemented in the transition-state tools module for VASP.[32] All reported states in the potential energy diagram are zero-point energy-corrected. Transition states in the dissociative adsorption of CO_2 were corroborated by vibrational frequency analysis.

3. RESULTS

3.1. AP-XPS Measurements. Figure 1 shows the evolution of the O 1s spectrum as the surface is exposed to

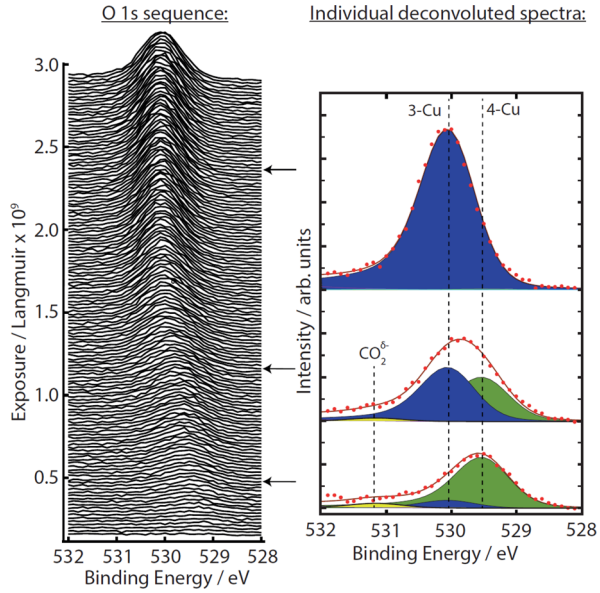

Figure 1. Measured O 1s sequence as the surface is exposed to 300 mTorr of CO_2 at a temperature of 370 K. The right side of the figure shows examples of deconvoluted spectra.

300 mTorr CO_2 at 370 K. Upon CO_2 exposure, a coverage of atomically adsorbed oxygen starts to appear, originating from CO_2 dissociation. Initially, the spectrum consists of one peak at 529.5 eV. As the oxygen coverage increases, the peak is observed to shift toward higher binding energy, reaching 530.0 eV at the saturation coverage of 0.5 ML. As reported by Eren et al.,[11] there is an additional peak at ∼531 eV, corresponding to adsorbed $CO_2^{\delta-}$. Under the current conditions, however, the corresponding coverage of this species is never above 0.02 ML, and as the O coverage increases, this peak, if present, is hidden in the tails of the O peaks. Hence, we do not draw any conclusions concerning the presence of the adsorbed CO_2 from these measurements, but refer to the study by Eren et al., who reported adsorbed CO_2 at low O coverages but not at 0.3 ML at room temperature.

We have in a recently published study[23] concluded that, up to a coverage of 0.25 ML, the adsorbed oxygen forms a disordered p(2 × 2) phase, with oxygen in fourfold hollow sites. This structure converts into a missing row reconstruction, where each O atom is coordinated to three Cu atoms.[23] The calculated O 1s core level shift between four- and threefold coordinated O atoms is 0.7 eV, which is in good agreement with the measured shift of 0.5 eV in Figure 1. With the two peaks at 529.5 and 530.0 eV assigned to be oxygen at the unreconstructed and reconstructed part of the surface,

DOI: 10.1021/jacs.8b07906
J. Am. Chem. Soc. 2018, 140, 12974−12979

respectively, the individual spectra of the O 1s sequence in Figure 1 can be deconvoluted using these peaks. Such an analysis is shown to the right in Figure 1 for three cases.

The integrated intensities of the peaks at 529.5 and 530.0 eV, as well as their sum, for the entire series of spectra are shown in Figure 2. We find that the oxygen uptake curve can

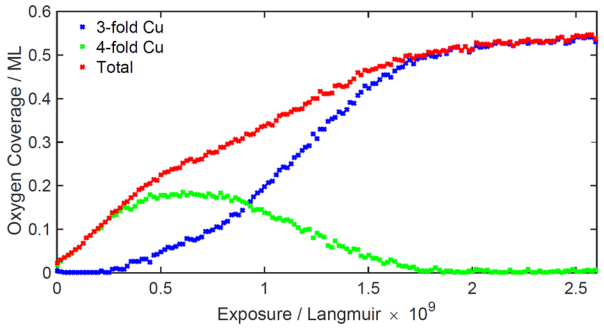

Figure 2. Evolution of adsorbed oxygen from CO_2. The two peaks at 529.5 eV (green dots) and 530 eV (blue dots) are fitted for the entire series of spectra in Figure 1. The coverage is estimated by normalizing the integrated intensities to the MR structure.

be characterized by three regions: (i) A linear region in the coverage range up to 0.25 ML, (ii) another linear region with a gentler slope up to a coverage of 0.45 ML, and (iii) an exponentially decaying increase up to the saturation coverage of 0.5 ML. A linear uptake curve indicates that the rate of dissociative adsorption is constant and the number of sites responsible for dissociation does not depend on coverage. The change in slope at 0.25 ML shows that the rate constant is lowered by the presence of oxygen, although the active sites remain unoccupied. These effects are corroborated by the DFT calculations.

3.2. DFT Calculations. *3.2.1. Dissociative Adsorption of CO_2 on Cu(100).* The calculated energy landscape for the dissociation of CO_2 over Cu(100) is shown in Figure 3. In agreement with previous reports,[22] we find that CO_2 adsorbs as a bent activated $CO_2^{\delta-}$ species. This is a crucial step for the dissociation process as C−O bond cleavage from linear CO_2 is associated with a barrier of ∼3 eV. The adsorption is endothermic by 0.43 eV on the pristine surface, with respect to CO_2 in the gas phase, and has an energy barrier of 0.55 eV. This barrier is associated with both the cost of the charge transfer from the surface to the molecule and the structural distortion of the molecule and the surface. To complete the dissociation, the activated $CO_2^{\delta-}$ is elongated and the C−O bond is broken over the adjacent bridge site. The dissociation step has a barrier of 0.83 eV and is endothermic by 0.02 eV with respect to adsorbed $CO_2^{\delta-}$. A configuration of CO* + O* is left at the surface, where the CO* molecule occupies the initial bridge site, while the oxygen atom occupies a fourfold hollow site. The CO molecule is adsorbed to the surface by 0.97 eV. Note that the barrier for desorption of CO_2 from the $CO_2^{\delta-}$ configuration is only 0.12 eV. The entropy difference between CO_2 in the gas phase and CO in the gas phase with adsorbed O is ∼0.08 eV in favor of CO_2. The endothermic nature of the reaction explains the high pressure needed to drive the reaction.

The effect of adsorbed O on the CO_2 dissociation was investigated through a systematic test of the stability of

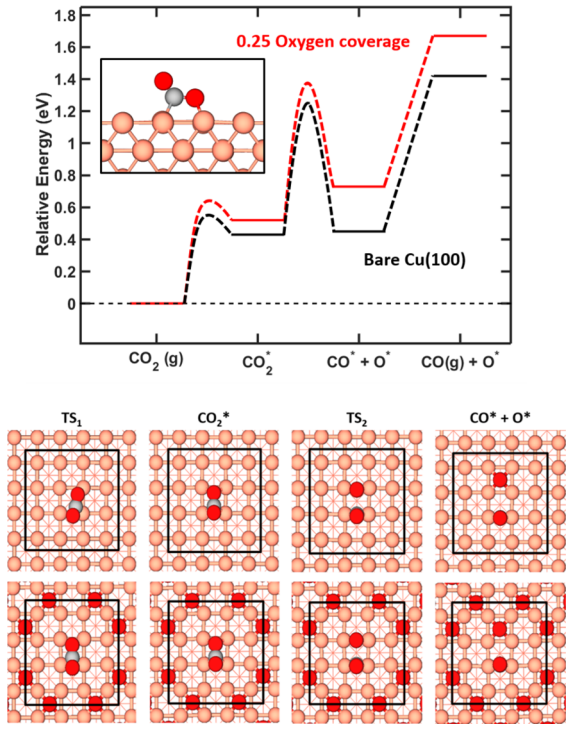

Figure 3. CO_2 dissociation on pristine and O-covered Cu(100). The upper panel shows the zero-point-corrected energy diagram of the two-step dissociative adsorption process. The inset shows adsorbed CO_2. The lower panel shows the atomic models of the dissociative process on both the pristine and O-covered Cu(100). The c(4 × 4) surface cell is indicated by black lines. Atomic color codes: Cu (pink), O (red), and C (light gray).

activated $CO_2^{\delta-}$ at an oxygen coverage of 0.083 ML. All eight possible nonequivalent configurations of CO_2 and oxygen co-adsorption in a c(4 × 3) surface cell were explored; see Figure 4. We find that the stability of CO_2 on the O-covered surface is

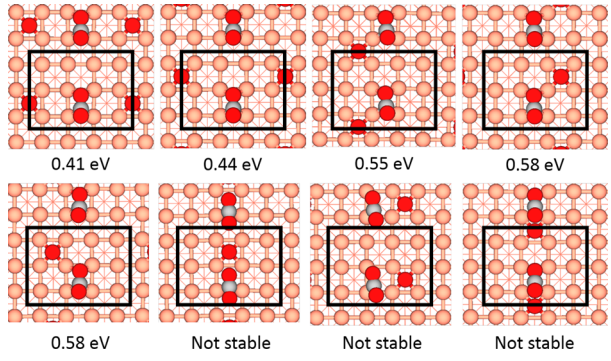

Figure 4. CO_2 on Cu(100) with preadsorbed oxygen. The (endothermic) adsorption energy with respect to CO_2 in the gas phase is indicated. The c(3 × 4) surface cell is indicated by black lines. Color codes as in Figure 3.

sensitive to its relative position with respect to the adsorbed oxygen atoms. Especially, it is shown that the available number of sites for CO_2 is reduced significantly with a coverage of oxygen.

At a coverage of 0.25 ML, oxygen is predicted to form a p(2 × 2) adsorption structure.[23] According to our calculations, the chemisorbed bent $CO_2^{\delta-}$ is not stable on this surface, which

DOI: 10.1021/jacs.8b07906
J. Am. Chem. Soc. 2018, 140, 12974−12979

suggests that the O coverage should saturate at 0.25 ML instead of 0.5 ML as observed experimentally (Figure 2). CO_2 may adsorb at a 0.25 ML oxygen coverage provided that the O atoms are clustered. We have considered such a configuration in Figure 3. This structure is only 0.09 eV higher in binding energy than the p(2 × 2) and might form at 370 K.[23] The structure is similar to the c(4 × 6) presented by Fujita et al.[33] CO_2 has a stable minimum when adsorbed on this structure, with an endothermic adsorption energy of 0.52 eV, which is roughly 0.1 eV higher than for the pristine surface. Although these calculations indicate that CO_2 may dissociate at Cu(100) with an O coverage higher than 0.25 ML, this possibility does not provide any explanation for the linear uptake curve as the number of sites for dissociation should decrease monotonously.

3.2.2. CO_2 Dissociation on Stepped Surface. To find an explanation for the linear uptake curve, we have investigated the dissociative adsorption of CO_2 over the stepped copper surface. As the close-packed (111) steps are expected to be the more dominant step,[34] we chose to study a Cu(611) surface, which has a surface unit cell comprising two (100) terraces separated by a (111) step. Figure 5 shows the corresponding

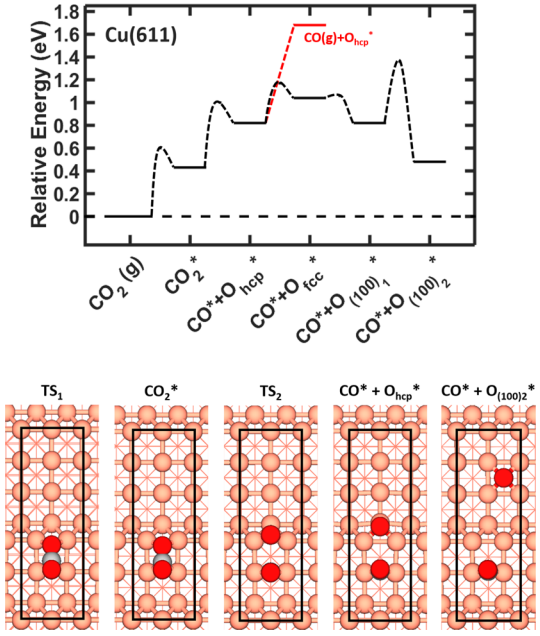

Figure 5. CO_2 dissociation on pristine Cu(611). The upper panel shows the zero-point-corrected energy diagram of the two-step dissociative adsorption process. The lower panel shows the atomic models of the dissociative process on Cu(611). The surface cell is indicated by black lines. Color codes as in Figure 3.

energy landscape and models. The dissociation process is similar to the one at Cu(100), proceeding through adsorbed $CO_2^{\delta-}$ with subsequent elongation and breaking of the C−O bond over the step. Atomic oxygen is transferred over the bridge site to occupy a threefold hollow site below the step, while CO* remains on the initial bridge site. The barrier for adsorption is slightly higher than that on Cu(100): 0.60 eV instead of 0.55 eV. The activated CO_2 has, however, the same endothermicity as on Cu(100). Dissociation of $CO_2^{\delta-}$ has a barrier of 0.57 eV and (CO* + O*) configuration is endothermic by 0.39 eV with respect to the activated CO_2. However, diffusion of O from the threefold hollow site at the step to a fourfold position on the (100) terrace makes $CO_2^{\delta-}$ and the (CO* + O*) isoenergetic.

The barrier for CO_2 dissociation from the adsorbed state is 0.26 eV lower on the step as compared to the (100) terrace. Additionally, the barrier for CO_2 desorption is slightly higher: 0.17 eV as compared to 0.12 eV. With use of the Arrhenius expression, these differences give, at 370 K, a higher probability of CO_2 dissociation on Cu(611) as compared to that on Cu(100) by 4 orders of magnitude; see Supporting Information.

In addition to lowering of the dissociation barrier, steps enable a facile separation between adsorbed CO and O. This is an important aspect as the barrier for CO and O recombination is lower than the barriers associated with diffusion of O to the terrace sites. From the threefold hollow site on the step, which is the position of O after dissociation, there is a sequence of three barriers for O to diffuse out on the lower terrace. The highest of these barriers is 0.54 eV, whereas the barrier for O diffusion on Cu(100) is 0.80 eV.

3.2.3. Avoiding Poisoning of Step Sites. Preferential CO_2 dissociation at steps would rationalize the linear uptake curves provided that the steps are not poisoned by the reaction products. Importantly, there is a thermodynamic driving force for oxygen to diffuse away from the step and instead occupy sites on the terraces. This is exemplified by calculating the stability of p(2 × 2) and c(2 × 2) types of structures on Cu(11 1 1) (Figure 6). The oxygen coverage in the two cases is 0.25

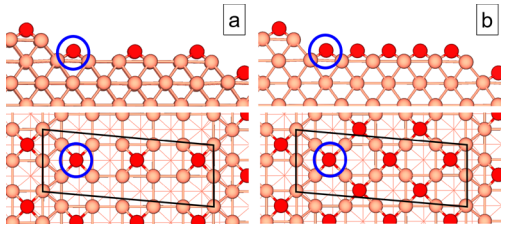

Figure 6. p(2 × 2) (a) and c(2 × 2) (b) types of structures on Cu(11 1 1). The circle highlights the oxygen atom adsorbed right below the step for which differential adsorption energies are calculated. The surface cell is indicated by black lines. Color codes as in Figure 3.

and 0.42 ML, respectively. For p(2 × 2), this is the same coverage as on the extended surface whereas the c(2 × 2) structure has a coverage of 0.5 ML on Cu(100). On Cu(11 1 1), the average oxygen binding energy is −1.86 and −1.74 eV for the low- and high-coverage case, respectively. This should be compared to the corresponding binding energies on Cu(100), which are −2.02 and −1.77 eV. The considerable reduction in stability is related to the occupation of the fourfold site below the step. The differential binding energy for this site is −1.63 and −1.32 eV for the p(2 × 2) and c(2 × 2) types of structures, respectively. The reduced binding energies on the Cu(11 1 1) surface can partly be attributed to compressive strain as Cu−Cu bond distances are reduced in the topmost surface layer.

When the coverage increases, oxygen resulting from dissociation processes on one step will by diffusion eventually reach the next lower step. This is expected to happen when the coverage approaches 0.25 ML, that is, when the surface is covered by a p(2 × 2) structure. As for Cu(100), this would block the adsorption of CO_2 and, thereby, hinder the reaction.

DOI: 10.1021/jacs.8b07906
J. Am. Chem. Soc. 2018, 140, 12974−12979

Still the dissociation is measured to continue until a coverage of 0.5 ML has been reached. The reason for this is most likely that the step is kept free from O through reaction with CO. As long as the dissociation rate is high enough relative to the O diffusion rate, and considering the high barrier for CO desorption, there will always be CO from another dissociation event available for reaction with the O that, by diffusion, reaches the active step sites. This will, of course, result in continuous removal of some O, and a reduced increase of the O coverage. This scenario is consistent with the change of the slope of the uptake curve when the coverage approaches 0.25 ML.

4. DISCUSSION

On the basis of our combined AP-XPS and DFT results, we suggest a model for the dissociative adsorption of CO_2 on Cu(100), where dissociation on steps dominate. The effect of the steps is twofold, both lowering the activation barrier for the dissociation and separating the resulting O and CO, thus hindering recombination. This scenario agrees with the linear behavior of the O uptake. A similar importance of steps has previously been suggested by Somorjai et al., for adsorption of CO_2 on Cu(311).[17]

In addition, our model is consistent with previous reports, of which the recent combined AP-XPS and HP-STM study by Eren et al. is of special interest.[11] Eren et al. show that CO_2 is able to adsorb on the clean Cu(100) surface; while at an O coverage of 0.3 ML, the CO_2 coverage is below the detection limit. This agrees well with our DFT calculations showing that the adsorption of CO_2 is efficiently blocked by adsorbed O such that no CO_2 adsorption can occur on the p(2 × 2) structure found to be the stable phase at 0.25 ML coverage.

The O coverage increases above 0.3 ML in both Eren's and our studies, suggesting that the adsorbed CO_2 found by AP-XPS is not involved in the reaction. This problem is solved by the reaction taking place on steps rather than the terraces, given that oxygen diffuses away from the active sites.

Another detail to take into account is that different studies have shown significantly different adsorption rates. According to ref 11, similar exposures of Cu(100) to 0.3 Torr CO_2 at room temperature for approximately 3 min at ALS Beamlines 9.3.2 and 11.0.2 results in 0.34 and 0.48 ML O coverage, respectively. This was attributed to different background pressures in the experimental chambers. We made a similar exposure for approximately 20 min, also at Beamline 9.3.2, resulting in an O coverage of about 0.06 ML; see Supporting Information. We do not believe that this large difference can be explained by the experimental environment, especially since the experiments were performed at the same beamline. Instead, we believe that the difference is due to the reaction occurring at steps since the step density depends strongly on the sample preparation.

5. CONCLUSIONS

We have studied the dissociation of CO_2 over the Cu(100) using AP-XPS and DFT. Our results show that CO_2 adsorbs dissociatively on Cu(100) with a resulting O uptake that is initially unaffected by the O coverage. This is incompatible with CO_2 adsorbing on the (100) terraces, as O would block the adsorption, resulting in a gradually reduced uptake rate. Instead, we propose a model where dissociation on surface steps completely dominate. In this scenario, the steps both lower the activation barrier for the dissociation and separate the resulting CO and O, thus hindering recombination. Furthermore, there is a thermodynamic driving force for the resulting O to diffuse away from the steps out on the terrace, leaving the active step sites available for further adsorption.

Our results emphasize the importance of steps in CO_2 hydrogenation catalysis and form a basis for further studies to establish the roles of Cu, ZnO, and the Cu/ZnO interface in industrial catalysts. Such fundamental understanding is, in turn, a prerequisite for a rational design of future catalysts aimed at reducing the emission of greenhouse gases into the atmosphere.

■ ASSOCIATED CONTENT

Supporting Information

The Supporting Information is available free of charge on the ACS Publications website at DOI: 10.1021/jacs.8b07906.

STM and LEED image of the missing row reconstruction, additional AP-XPS spectra, and a comparison between the theoretical dissociation rates on Cu(100) and Cu(611) (PDF)

■ AUTHOR INFORMATION

Corresponding Author

*johan.gustafson@sljus.lu.se

ORCID

Andreas Schaefer: 0000-0001-6578-5046
Anders Hellman: 0000-0002-1821-159X
Edvin Lundgren: 0000-0002-3692-6142
Henrik Grönbeck: 0000-0002-8709-2889
Johan Gustafson: 0000-0003-3325-0658

Author Contributions

#Benjamin Hagman and Alvaro Posada-Borbón have contributed equally to this article.

Notes

The authors declare no competing financial interest.

■ ACKNOWLEDGMENTS

The authors thank the Knut and Alice Wallenberg Foundation (No.: KAW 2015.0058), the Swedish Research Council, and the Swedish Foundation for Strategic Research for financial support. This work is done within the Röntgen-Ångström collaboration "Time-resolved in situ methods for design of catalytic sites within sustainable chemistry". The staff at the ALS are gratefully acknowledged. This research used resources of the Advanced Light Source, which is a DOE Office of Science User Facility under contract no. DE-AC02-05CH11231. The calculations have been performed at C3SE (Göteborg) through a SNIC grant.

■ REFERENCES

(1) Wang, W.; Wang, S.; Ma, X.; Gong, J. Recent advances in catalytic hydrogenation of carbon dioxide. *Chem. Soc. Rev.* **2011**, *40*, 3703−3727.

(2) Porosoff, M. D.; Yan, B.; Chen, J. G. Catalytic reduction of CO_2 by H_2 for synthesis of CO, methanol and hydrocarbons: challenges and opportunities. *Energy Environ. Sci.* **2016**, *9*, 62−73.

(3) Behrens, M.; Studt, F.; Kasatkin, I.; Kühl, S.; Hävecker, M.; Abild-Pedersen, F.; Zander, S.; Girgsdies, F.; Kurr, P.; Kniep, B. L.; Tovar, M.; Fischer, R. W.; Nørskov, J. K.; Schlögl, R. The Active Site of Methanol Synthesis over $Cu/ZnO/Al_2O_3$ Industrial Catalysts. *Science* **2012**, *336*, 893−897.

DOI: 10.1021/jacs.8b07906
J. Am. Chem. Soc. 2018, 140, 12974−12979

(4) Nakamura, J.; Nakamura, I.; Uchijima, T.; Kanai, Y.; Watanabe, T.; Saito, M.; Fujitani, T. A Surface Science Investigation of Methanol Synthesis over a Zn-Deposited Polycrystalline Cu Surface. *J. Catal.* **1996**, *160*, 65−75.
(5) Nakamura, J.; Choi, Y.; Fujitani, T. On the Issue of the Active Site and the Role of ZnO in Cu/ZnO Methanol Synthesis Catalysts. *Top. Catal.* **2003**, *22*, 277−285.
(6) Palomino, R. M.; Ramírez, P. J.; Liu, Z.; Hamlyn, R.; Waluyo, I.; Mahapatra, M.; Orozco, I.; Hunt, A.; Simonovis, J. P.; Senanayake, S. D.; Rodriguez, J. A. Hydrogenation of CO_2 on ZnO/Cu(100) and ZnO/Cu(111) Catalysts: Role of Copper Structure and Metal-Oxide Interface in Methanol Synthesis. *J. Phys. Chem. B* **2018**, *122*, 794−800.
(7) Kattel, S.; Ramírez, P. J.; Chen, J. G.; Rodriguez, J. A.; Liu, P. Active sites for CO_2 hydrogenation to methanol on Cu/ZnO catalysts. *Science* **2017**, *355*, 1296−1299.
(8) Nakamura, J.; Fujitani, T.; Kuld, S.; Helveg, S.; Chorkendorff, I.; Sehested, J. Comment on Active sites for CO_2 hydrogenation to methanol on Cu/ZnO catalysts. *Science* **2017**, *357*, eaan8074.
(9) Kattel, S.; Ramírez, P. J.; Chen, J. G.; Rodriguez, J. A.; Liu, P. Response to Comment on Active sites for CO2 hydrogenation to methanol on Cu/ZnO catalysts. *Science* **2017**, *357*, eaan8210.
(10) Rasmussen, P. B.; Taylor, P. A.; Chorkendorff, I. The interaction of carbon dioxide with Cu(100). *Surf. Sci.* **1992**, *269-270*, 352−359.
(11) Eren, B.; Weatherup, R. S.; Liakakos, N.; Somorjai, G. A.; Salmeron, M. Dissociative Carbon Dioxide Adsorption and Morphological Changes on Cu(100) and Cu(111) at Ambient Pressures. *J. Am. Chem. Soc.* **2016**, *138*, 8207−8211.
(12) Favaro, M.; Xiao, H.; Cheng, T.; Goddard, W. A.; Yano, J.; Crumlin, E. J. Subsurface oxide plays a critical role in CO_2 activation by Cu(111) surfaces to form chemisirbed CO_2, the first step in reduction of CO_2. *Proc. Natl. Acad. Sci. U. S. A.* **2017**, *114*, 6706−6711.
(13) Bonicke, I. A.; Kirstein, W.; Thieme, F. A Study on CO_2 dissociation on a stepped (332) copper surface. *Surf. Sci.* **1994**, *307−309*, 177−181.
(14) Schneider, T.; Hirschwald, W. Interaction of Carbon dioxide with clean and oxygenated Cu(110) surfaces. *Catal. Lett.* **1992**, *14*, 197−205.
(15) Nakamura, J.; Rodriguez, J. A.; Campbell, C. T. Does CO_2 dissociatively adsorb on Cu surfaces? *J. Phys.: Condens. Matter* **1989**, *1*, 149−160.
(16) Funk, S.; Hokkanen, B.; Wang, J.; Burghaus, U.; Bozzolo, G.; Garcés, J. E. Adsorption dynamics of CO_2 on Cu(110): A Molecular beam study. *Surf. Sci.* **2006**, *600*, 583−590.
(17) Fu, S.; Somorjai, G. Interactions of O_2, CO, CO_2, and D_2 with the stepped Cu(311) crystal face: comparison to Cu(110). *Surf. Sci.* **1992**, *262*, 68−76.
(18) Ernst, K.-H.; Schlatterbeck, D.; Christmann, K. Adsorption of carbon dioxide on Cu(110) and on hydriogen and oxygen covered Cu(110) surfaces. *Phys. Chem. Chem. Phys.* **1999**, *1*, 4105−4112.
(19) Koitaya, T.; Yamamoto, S.; Shiozawa, Y.; Takeuchi, K.; Liu, R.-Y.; Mukai, K.; Yoshimoto, S.; Akikubo, K.; Matsuda, I.; Yoshinobu, J. Real-Time Observation of Reaction Processes of CO_2 on Cu(997) by Ambient-Pressure X-ray Photoelectron Spectroscopy. *Top. Catal.* **2016**, *59*, 526−531.
(20) Bendavid, L. I.; Carter, E. CO_2 Adsorption on Cu_2O(111): A DFT+U and DFT-D Study. *J. Phys. Chem. C* **2013**, *117*, 26048−26059.
(21) Mishra, A. K.; Roldan, A.; de Leeuw, N. H. CuO Surfaces and CO_2 Activation: A Dispersion-Corrected DFT+U Study. *J. Phys. Chem. C* **2016**, *120*, 2198−2214.
(22) Liu, C.; Cundari, T. R.; Wilson, A. K. CO_2 Reduction on Transistion Metal (Fe, Co, Ni, and Cu) Surfaces: In Comparison with Homogeneous Catalysis. *J. Phys. Chem. C* **2012**, *116*, 5681−5688.
(23) Posada-Borbón, A.; Hagman, B.; Schaefer, A.; Zhang, C.; Shipilin, M.; Hellman, A.; Gustafson, J.; Grönbeck, H. Initial oxidation of Cu(100) studied by X-ray photo-electron spectroscopy and density functional theory calculations. *Surf. Sci.* **2018**, *675*, 64−69.
(24) Grass, M. E.; Karlsson, P. G.; Aksoy, F.; Lundqvist, M.; Wannberg, B.; Mun, B. S.; Hussain, Z.; Liu, Z. New ambient pressure photoemission endstation at Advanced Light Source beamline 9.3.2. *Rev. Sci. Instrum.* **2010**, *81*, 053106.
(25) Okada, M.; Hashinokuchi, M.; Fukuoka, M.; Kasai, T.; Moritani, K.; Teraoka, Y. Protective layer formation during oxidation of Cu_3 Au(100) using hyperthermal O_2 molecular beam. *Appl. Phys. Lett.* **2006**, *89*, 201912.
(26) Perdew, J. P.; Burke, K.; Ernzerhof, M. Generalized gradient approximation made simple. *Phys. Rev. Lett.* **1996**, *77*, 3865−3868.
(27) Kresse, G.; Hafner, J. *Ab initio* Molecular Dynamics for Liquid Metals. *Phys. Rev. B: Condens. Matter Mater. Phys.* **1993**, *47*, 558−561.
(28) Kresse, G.; Hafner, J. *Ab initio* molecular-dynamics simulations of the liquid-metal-amorphous-semiconductor transition in germanium. *Phys. Rev. B: Condens. Matter Mater. Phys.* **1994**, *49*, 14251−14269.
(29) Kresse, G.; Furthmüller, J. Efficenciey of ab-initio Total Energy Calculations for Metals and Semiconductors Using a Plane-Wave Basis Set. *Comput. Mater. Sci.* **1996**, *6*, 15−50.
(30) Kresse, G.; Furthmüller, J. Efficent Iterative Schemes for *ab initio* Total-Energy Calculations Using a Plane-Wave Basis Set. *Phys. Rev. B: Condens. Matter Mater. Phys.* **1996**, *54*, 11169−11186.
(31) Tran, F.; Laskowski, R.; Blaha, P.; Schwarz, K. Performance on molecules, surfaces, and solids of the Wu-Cohen GGA exchange-correlation energy functional. *Phys. Rev. B: Condens. Matter Mater. Phys.* **2007**, *75*, 115131.
(32) Henkelman, G.; Uberuaga, B. P.; Jonsson, H. A Climbing Image Nudged Elastic Band Method for Finding Saddle Points and Minimum Energy Paths. *J. Chem. Phys.* **2000**, *113*, 9901−9904.
(33) Fujita, T.; Okawa, Y.; Matsumoto, Y.; Tanaka, K. Phase boundaries of nanometer scale c(2 × 2)-O domains on the Cu(100) surface. *Phys. Rev. B: Condens. Matter Mater. Phys.* **1996**, *54*, 2167−2174.
(34) Liu, C.-L. Energetics of diffusion processes during nucleation an growth for the Cu/Cu(100) system. *Surf. Sci.* **1994**, *316*, 294−302.

DOI: 10.1021/jacs.8b07906
J. Am. Chem. Soc. 2018, 140, 12974−12979